NUCL SCI TECH (2020) 31:50
https://doi.org/10.1007/s41365-020-00760-3

Evaluation of cosmogenic activation of copper and germanium during production in Jinping Underground Laboratory

Wei-He Zeng[1,2] · Hao Ma[1,2] · Ming Zeng[1,2] · Zhi Zeng[1,2] · Qian Yue[1,2] · Jian-Ping Cheng[1,2,3] · Jun-Li Li[1,2]

Received: 10 February 2020 / Revised: 11 March 2020 / Accepted: 17 March 2020 / Published online: 4 May 2020

Abstract Intrinsic radiation of materials is one of the major backgrounds for many rare-event search experiments. Thus, the production of pure materials in an underground laboratory is a promising approach for eliminating cosmogenic radionuclides. In this paper, we demonstrate a procedure to evaluate the yields of cosmogenic radionuclides in copper and germanium in the second phase of the China Jinping Underground Laboratory. Our results show that for copper and germanium materials, the largest cosmogenic background comes from ^{3}H and ^{57,58,60}Co, and ^{3}H and ^{68}Ge, respectively, which all have yields on the order of 10^{-7} kg^{-1} day^{-1}. The corresponding radioactivities after 90 days pf exposure underground are estimated to be lower than 10^{-6} μBq kg^{-1}.

Keywords Cosmic rays · Cosmogenic radionuclides · Underground laboratory · Monte Carlo simulation

This work was supported by the National Natural Science Foundation of China (No. U1865205).

✉ Zhi Zeng
zengzhi@tsinghua.edu.cn

1 Department of Engineering Physics, Tsinghua University, Beijing 100084, China

2 Key Laboratory of Particle and Radiation Imaging (Tsinghua University), Ministry of Education, Beijing 100084, China

3 College of Nuclear Science and Technology, Beijing Normal University, Beijing 100875, China

1 Introduction

An ultralow-background environment is required in rare-event search experiments, because background events may cover the physical events of interest. Accordingly, most background-sensitive experiments are performed in underground laboratories to minimize the impact of cosmic rays. Among these underground laboratories, the China Jinping Underground Laboratory (CJPL) is the deepest currently in operation [1]. In addition, various types of passive or active shielding are applied to further reduce the background affecting these experiments. The shielding components and main detectors should be made of ultra-pure materials to ensure that they do not additionally contribute to the background.

Germanium is a common detector material for direct dark matter detection and neutrinoless double-decay experiments, including the China Dark Matter Experiment (CDEX), Coherent Germanium Neutrino Technology experiment, Super Cryogenic Dark Matter Search, Edelweiss experiment, Germanium Detector Array experiment, and MAJORANA Demonstrator [1–6]. In these experiments, cosmogenic radionuclides in the germanium introduce a significant proportion of background signals. For example, the Edelweiss-III experiment reported a measurement of cosmogenic tritium and other nuclides in their germanium detectors [4]. The CDEX collaboration predicted the cosmogenic activation of germanium detectors manufactured at sea level for future ton-scale experiments [7]. In addition, copper, especially oxygen-free high thermal conductivity copper, is widely used as the shielding material closest to the active detectors in these experiments owing to its high chemical purity and mechanical strength.

However, it has the same problem of cosmogenic activation.

One approach to eliminate the cosmogenic radionuclides in copper and germanium is to grow the crystals in underground laboratories, which are shielded from most cosmic rays. The second phase of CJPL (CJPL-II) is under construction, and the civil construction part of the project is almost complete. Dark matter detection and other experiments will soon be running in CJPL-II. The production of ultrapure copper and germanium directly in CJPL-II has been proposed. In this work, we develop a method of evaluating the cosmogenic background for copper and germanium in the underground laboratory using experimental measurements, Monte Carlo simulations, and theoretical calculations.

2 Methods

2.1 Muon source measurement and simulation

To simulate cosmogenic activation in an underground laboratory, it is necessary to know the flux and energy of cosmic rays at that depth. We combine experimental measurements and a Monte Carlo simulation to obtain this information for cosmic rays in CJPL-II.

Muons are the dominant component of cosmic rays in the underground laboratory [8]. High-energy, highly penetrating muons arrive at the underground laboratory through approximately 2400 m of rock. The method of measuring the muon flux in CJPL-I has also been applied in CJPL-II [9]. The system consists of six plastic scintillation detectors, which are divided into two groups. The length, width, and height of each detector are 1, 0.5, and 0.05 m, respectively, and the effective detection area is 0.5 m^2. As shown in Fig. 1, each group consists of three stacked detectors, which form a triple-coincidence system that can distinguish cosmic muons from environmental radiation such as gamma-rays. The waveforms from the photomultiplier tubes in the plastic scintillators are also recorded to improve the background discrimination.

After environmental radiation is rejected and the triple-coincidence events (N) are counted, the muon flux (Φ_μ) of the measurement can be estimated using Eq. (1).

$$\Phi_\mu = \frac{N}{\varepsilon S t} \tag{1}$$

Here ε is the total efficiency of the detection system, S is the detection area of the detector, and t is the acquisition time of the measurement. Efficiency corrections in our system include the dead time, detection efficiency of the plastic scintillator, edge effect, and solid-angle correction of the triple-coincidence system. Owing to the structure of Jinping mountain, muons approaching from directly above the mountain encounter the smallest rock thickness; thus, the majority of detected muons have zenith angles close to 0 [9]. Additionally, the dead time is negligible, and the detection efficiency of the system is close to 1. Thus, the total efficiency ε is set to 1 in our calculation.

However, the measurement system cannot measure the energy of incident muons. We have simulated the residual muon flux and spectrum in the CJPL using the MUSIC code [10, 11]. That simulation models the Jinping mountain as a semi-sphere of standard rock with a radius of 2400 m, and the laboratory is located at the center of the mountain. The energy and angular distribution of muons before they penetrate the mountain are calculated using the Gaisser formula [12]. The simulated muon flux is compared with our measurement for validation, and the energy distribution of residual muons is utilized to simulate cosmic activation in CJPL-II.

2.2 Secondary particles in the laboratory

The secondary particles from muons in the underground laboratory are simulated using CERN's GEANT4 toolkit [13].

The experimental hall in CJPL-II is modeled as several boxes consisting of different materials (Fig. 2). From the outside to the inside, these are standard rock (2 m thick), concrete (20 cm thick), and a $50\,\text{m} \times 10\,\text{m} \times 10\,\text{m}$ experimental hall filled with air. We simulated a $25\,\text{m} \times 5\,\text{m} \times 0.4\,\text{m}$ copper or germanium plate 1 m above the ground in the center of the experimental hall.

The incident particles in the simulation are residual muons from cosmic rays. The initial kinetic energy of the muons is set to the average energy found in the MUSIC simulation. Furthermore, the positions of the incident muons are randomly generated from the upper surface of the rock box with zero zenith angle, assuming that the residual muon trajectories are almost perpendicular to the outer rock.

GEANT4 uses different physics models and the corresponding cross sections to define the interactions between incident particles and target materials. For any Monte Carlo simulation, it is essential to choose a physics model that adequately describes the processes in the simulation. However, computational efficiency should also be considered to balance the time consumption and simulation precision. To improve the precision of secondary particles and the production of radionuclides, we choose the QGSP_BERT_HP physics list in GEANT4, which implements the Quark–Gluon String Precompound model and uses the data-driven high-precision neutron cross section for neutrons with energies lower than 20 MeV.

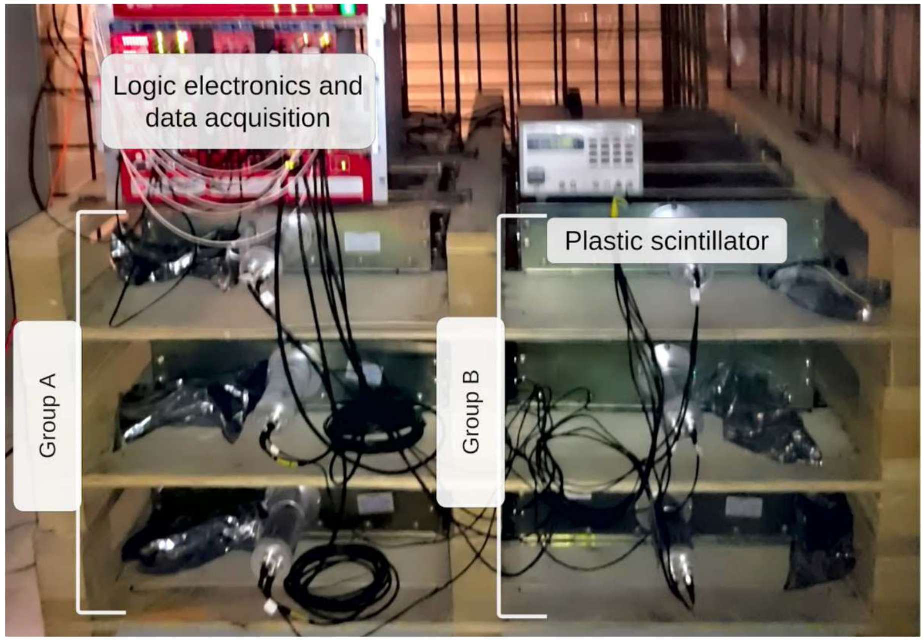

Fig. 1 (Color online) Photograph of the muon measurement system installed in CJPL-II

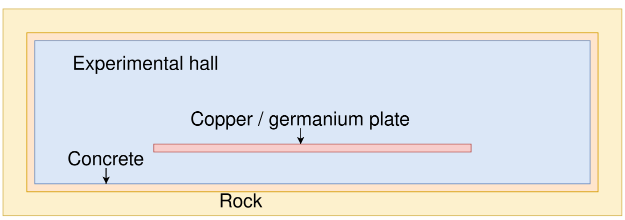

Fig. 2 (Color online) Model of the underground laboratory in the simulation (lateral view)

The track lengths and energies of secondary particles in the experimental hall, such as neutrons, protons, and gamma-rays, are recorded during the simulation. After the simulation results are normalized by the measured muon flux $\Phi\mu$, the secondary particle flux at an energy E is expressed by Eq. (2).

$$\Phi_{\mathrm{par}}(E) = \frac{l_{\mathrm{par}}(E)}{V \times t_{\mathrm{sim}}} = \frac{l_{\mathrm{par}}(E)}{V \times \dfrac{N_{\mathrm{sim}}}{\Phi\mu S_{\mathrm{sim}}}} \tag{2}$$

Here $l_{\mathrm{par}}(E)$ is the accumulated track length of secondary particles at E, V is the total volume of the experimental hall, N_{sim} is the number of incident muons, t_{sim} is the time needed to produce N_{sim} muons when the flux is $\Phi\mu$, and S_{sim} is the area of the rock box's upper surface, where muons are randomly sampled.

2.3 Production of radionuclides in copper and germanium

Because the copper or germanium material is modeled as a plate in the simulation geometry, radionuclides generated in the plate by primary muons or secondary particles can be counted during the simulation. The nuclide yields ($Y_{\mathrm{nuc,sim}}$) are then derived, as shown in Eq. (3).

$$Y_{\mathrm{nuc,sim}} = \frac{N_{\mathrm{nuc,sim}}}{m_{\mathrm{plate}} t_{\mathrm{sim}}} \tag{3}$$

$N_{\mathrm{nuc,sim}}$ is the number of nuclides of a certain type that are produced in the simulation, m_{plate} is the total mass of the plate, and t_{sim} is the simulated time described above for Eq. (2).

Owing to the computational complexity of the simulation and the low radionuclide production rate in the target materials, the statistical uncertainty is not optimal in this simulation scenario. We apply an alternative approach to verify and compare the results. Because neutrons are the main source of the radioactive activation, and the secondary neutron flux from muon interactions is recorded in the simulation, the radionuclide yield ($Y_{\mathrm{nuc,cal}}$) can be calculated using Eq. (4).

$$Y_{\mathrm{nuc,cal}} = \sum_{\mathrm{tar}} \frac{N_{\mathrm{A}} f_{\mathrm{tar}}}{A_{\mathrm{tar}}} \int \Phi_{\mathrm{n}}(E) \sigma_{\mathrm{tar,nuc}}(E) \mathrm{d}E \tag{4}$$

$\Phi_{\mathrm{n}}(E)$ is the simulated neutron flux spectrum, $\sigma_{\mathrm{tar,nuc}}(E)$ is the total cross section of the target nuclides that generate the radionuclides of interest, N_{A} is Avogadro's number, f_{tar} is the fraction of each nuclide in the target material, and A_{tar} is the atomic mass of the target nuclides. The cross sections used in the calculation are obtained using semi-empirical formulae and the ACTIVIA code [14], which is a computer package that calculates target—product cross sections using data tables.

From the simulated or calculated yields (Y), the activity (A) for an isotope with decay constant λ after the copper or germanium crystals are placed in the underground laboratory can be calculated for a specific exposure time (t_{exp}).

$$A = Y(1 - \mathrm{e}^{-\lambda t_{\mathrm{exp}}}) \tag{5}$$

3 Results

The results obtained after approximately 655 days of continuous operation of the muon detection system are listed in Table 1. The results from the two groups of detectors were combined, and the obtained flux of cosmic muons in CJPL-II was found to be $(2.01 \pm 0.19) \times 10^{-6}\ \mathrm{m}^{-2}\mathrm{s}^{-1}$, or $(63.5 \pm 5.9)\ \mathrm{m}^{-2}\mathrm{year}^{-1}$. The system is still running to obtain more data and reduce the statistical uncertainty.

According to a previous calculation [10], the average energy of muons reaching the CJPL is 369 GeV. We used GEANT4 to simulate 10^6 muons with that energy entering the CJPL-II model and obtained the cosmogenic neutron and proton flux spectra shown in Fig. 3. On the basis of the measured muon flux of $2.01 \times 10^{-6}\ \mathrm{m}^{-2}\mathrm{s}^{-1}$, the total fluxes of cosmogenic neutrons and protons are $6.53 \times 10^{-7}\ \mathrm{m}^{-2}\mathrm{s}^{-1}$ and $5.33 \times 10^{-9}\ \mathrm{m}^{-2}\mathrm{s}^{-1}$, respectively. Thus, secondary neutrons dominate the incident particles according to the cosmogenic activation calculation.

In comparison with the measured neutron background in CJPL-I [15] (Fig. 4), the simulation result shows a neutron flux five to six orders of magnitude lower than the total neutron background, which suggests that cosmogenic neutrons are not the major component of the neutron background at an underground site at the depth of the CJPL depth.

The simulated and calculated cosmogenic radionuclides affecting copper and germanium production in CJPL-II are listed in Tables 2 and 3, respectively. The yields at sea level calculated by ACTIVIA [14] are also presented for comparison. The yields from the simulation and calculation

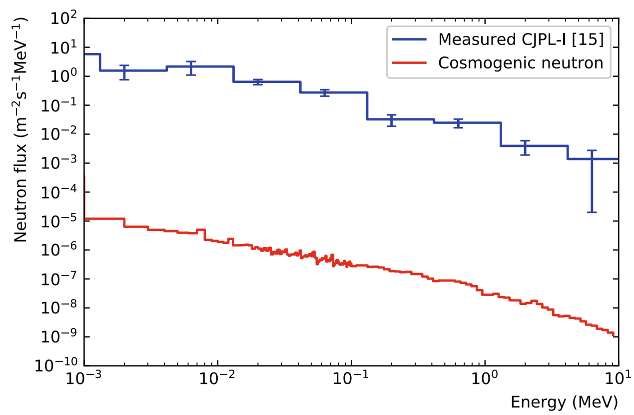

Fig. 4 (Color online) Comparison of the measured total neutron spectrum and simulated cosmogenic neutron spectrum

Table 1 Measured muon flux in CJPL-II

Group	Muon events	Time (s)	Flux ($\mathrm{m}^{-2}\mathrm{s}^{-1}$)	Statistical uncertainty ($\mathrm{m}^{-2}\mathrm{s}^{-1}$)
A	55	56,605,762	1.94×10^{-6}	0.26×10^{-6}
B	59	56,605,762	2.08×10^{-6}	0.27×10^{-6}
Average			2.01×10^{-6}	0.19×10^{-6}

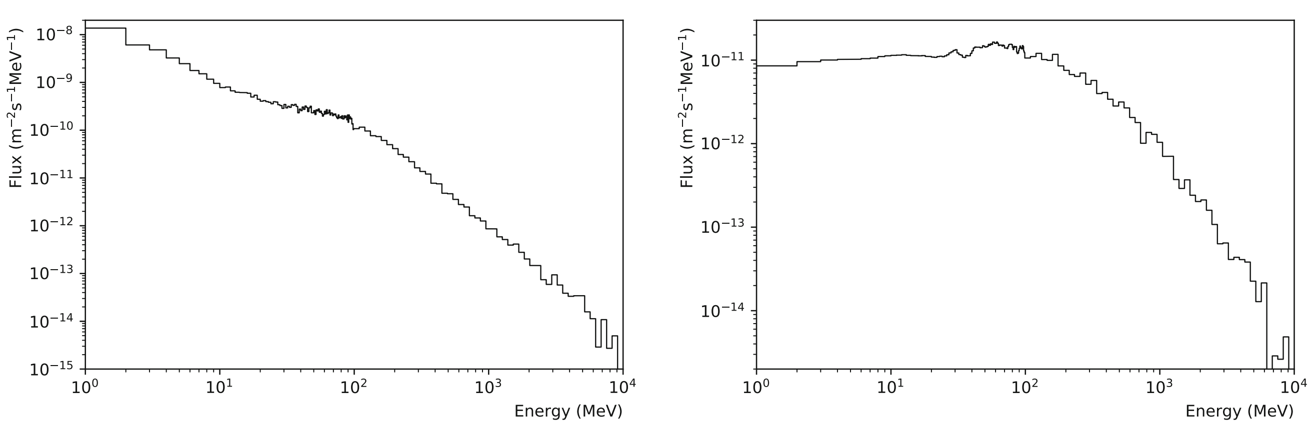

Fig. 3 Simulated secondary particle spectra (left: neutrons, right: protons) of experimental hall

Table 2 Yields of cosmogenic radionuclides in copper at CJPL-II and sea level

Nuclide	CJPL-II (simulation)	Statistical uncertainty	CJPL-II (calculation)	Sea level (ACTIVIA)
	Nuclide yields ($kg^{-1}day^{-1}$)			
^{3}H	1.04E−07	4.30E−09	4.13E−08	3.59E+01
^{56}Co	1.53E−08	1.65E−09	1.71E−08	8.74E+00
^{57}Co	8.68E−08	3.93E−09	6.84E−08	3.24E+01
^{58}Co	7.72E−08	3.70E−09	1.26E−07	5.66E+01
^{60}Co	8.87E−08	3.97E−09	6.60E−08	2.63E+01
^{59}Fe	1.71E−08	1.74E−09	9.96E−09	4.24E+00
^{54}Mn	2.22E−08	1.99E−09	2.35E−08	1.43E+01
^{46}Sc	3.02E−09	7.33E−10	2.58E−09	3.13E+00
^{65}Zn	4.80E−09	9.24E−10	1.18E−07	1.96E+01

Table 3 Yields of cosmogenic radionuclides in germanium at CJPL-II and sea level

Nuclide	CJPL-II (simulation)	Statistical uncertainty	CJPL-II (calculation)	Sea level (ACTIVIA)
	Nuclide yields ($kg^{-1}day^{-1}$)			
^{3}H	7.52E−08	3.66E−09	3.68E−08	3.41E+01
^{56}Co	3.37E−09	7.75E−10	1.38E−09	1.78E+00
^{57}Co	6.93E−09	1.11E−09	5.18E−09	6.30E+00
^{58}Co	6.40E−09	1.07E−09	6.68E−09	7.94E+00
^{60}Co	3.20E-−09	7.54E−10	2.46E−09	2.67E+00
^{55}Fe	9.07E−09	1.27E−09	2.32E−09	3.25E+00
^{68}Ge	2.47E−07	6.64E−09	2.20E−08	1.02E+01
^{54}Mn	3.02E−09	7.33E−10	1.61E−09	2.53E+00
^{63}Ni	1.11E−08	1.40E−09	1.73E−09	1.41E+00
^{65}Zn	6.21E−08	3.32E−09	3.43E−08	1.93E+01

for CJPL agree within an order of magnitude for most nuclides, except for ^{65}Zn in copper, and ^{63}Ni and ^{68}Ge in germanium. The inconsistency may result from the differences between the cross sections in ACTIVIA and the physics models in GEANT4. For example, the cross section for ^{65}Zn activation in ^{65}Cu at 100 MeV is 9.8 mb in ACTIVIA, whereas the corresponding value is 0.7 mb in our simulation. A comparison of the yields of cosmogenic radionuclides at CJPL and sea level reveals that shielding by Jinping mountain can reduce the radionuclide production by six to eight orders of magnitude.

Using Eq. 5 and the calculated yields in Tables 2 and 3, we calculated the radiation activities of cosmogenic radionuclides in copper and germanium grown in the CJPL after 30, 60, and 90 days. The results are presented in Tables 4 and 5, respectively.

Table 4 Activities of cosmogenic radionuclides in copper after exposure at CJPL-II

Nuclide	30 days	60 days	90 days
	Activity ($\mu Bq\,kg^{-1}$)		
^{3}H	2.20E−09	4.40E−09	6.58E−09
^{56}Co	4.67E−08	8.23E−08	1.10E−07
^{57}Co	5.83E−08	1.12E−07	1.62E−07
^{58}Co	3.72E−07	6.50E−07	8.57E−07
^{60}Co	8.22E−09	1.63E−08	2.43E−08
^{59}Fe	4.29E−08	6.97E−08	8.66E−08
^{54}Mn	1.75E−08	3.39E−08	4.92E−08
^{46}Sc	6.56E−09	1.17E−08	1.57E−08
^{65}Zn	1.12E−07	2.13E−07	3.07E−07

Table 5 Activities of cosmogenic radionuclides in germanium after exposure at CJPL-II

Nuclide	30 days	60 days	90 days
	Activity (μBq kg^{-1})		
^{3}H	1.96E−09	3.92E−09	5.86E−09
^{56}Co	3.78E−09	6.66E−09	8.87E−09
^{57}Co	4.42E−09	8.51E−09	1.23E−08
^{58}Co	1.96E−08	3.43E−08	4.53E−08
^{60}Co	3.06E−10	6.09E−10	9.09E−10
^{55}Fe	5.52E−10	1.10E−09	1.62E−09
^{68}Ge	1.88E−08	3.63E−08	5.25E−08
^{54}Mn	1.20E−09	2.32E−09	3.37E−09
^{63}Ni	1.12E−11	2.26E−11	3.38E−11
^{65}Zn	3.25E−08	6.22E−08	8.95E−08

4 Conclusion

To evaluate the advantages of growing copper and germanium in CJPL-II, we developed an estimation procedure based on experimental measurements, Monte Carlo simulations, and theoretical calculations. A triple-coincidence plastic scintillator detection system was used to measure the muon flux at CJPL-II. In addition, the energy of the muons was obtained from a previous simulation of muons penetrating Jinping mountain. The fluxes of secondary particles from muons in the experimental hall, as well as cosmogenic radionuclides in a simulated copper or germanium plate located in the experimental hall, were simulated using the GEANT4 toolkit. Additionally, the yields calculated from the simulated neutron flux and production cross sections were provided for validation.

The muon flux measurement indicates a significant reduction in cosmic rays due to shielding by Jinping mountain; the values are as low as $(63.5 \pm 5.9)\ \mathrm{m}^{-2}\mathrm{year}^{-1}$. Thus, the simulated fluxes of secondary particles from muons are negligible compared to the measured background neutrons in the CJPL, which are attributed mainly to environmental neutrons from the surrounding materials such as rock and concrete.

The simulated and calculated production of cosmogenic radionuclides in copper and germanium are in agreement. As expected, the radionuclide yields are approximately six to eight orders of magnitude lower than the yields at sea level. Moreover, the activities of most radionuclides after 90 days of exposure are less than 10^{-6} μ Bq kg^{-1}. Our results demonstrated that the cosmogenic radionuclide background at the CJPL is negligible compared to other potential background sources.

The estimation method developed in this work can be adapted for different underground laboratories and materials to ensure that the cosmogenic radionuclides at the site are negligible. In the future, the cosmic muons and environmental neutrons should be measured in a broader energy region. However, the development of radioassay technology is essential for obtaining quantitative concentrations of cosmogenic radionuclides in crystals grown in underground laboratories.

References

1. K.J. Kang, J.P. Cheng, J. Li et al., Introduction to the CDEX experiment. Front. Phys. **8**, 412–437 (2013). https://doi.org/10.1007/s11467-013-0349-1
2. C.E. Aalseth, P.S. Barbeau, J. Colaresi et al., CoGeNT: a search for low-mass dark matter using p-type point contact germanium detectors. Phys. Rev. D Part. Fields Gravit. Cosmol. **88**, 012002 (2013). https://doi.org/10.1103/PhysRevD.88.012002
3. R. Agnese, A.J. Anderson, T. Aramaki et al., Projected sensitivity of the SuperCDMS SNOLAB experiment. Phys. Rev. D **95**, 082002 (2017). https://doi.org/10.1103/PhysRevD.95.082002
4. E. Armengaud, Q. Arnaud, C. Augier et al., Measurement of the cosmogenic activation of germanium detectors in edelweiss-III. Astropart. Phys. **91**, 51–64 (2017). https://doi.org/10.1016/j.astropartphys.2017.03.006
5. M. Agostini, M. Allardt, A.M. Bakalyarov et al., Background-free search for neutrinoless double-β decay of ^{76}Ge with GERDA. Nature **544**, 47–52 (2017). https://doi.org/10.1038/nature21717
6. N. Abgrall, I.J. Arnquist et al., The Majorana demonstrator radioassay program. Nucl. Instrum. Methods Phys. Res. Sect. A Acc. Spectrom. Detect. Assoc. Equip. **828**, 22–36 (2016). https://doi.org/10.1016/j.nima.2016.04.070
7. J. Ma, Q. Yue, S. Lin et al., Study on cosmogenic activation in germanium detectors for future tonne-scale cdex experiment. Sci. China Phys. Mech. Astron. **62**, 11011 (2018). https://doi.org/10.1007/s11433-018-9215-0
8. C. Patrignani et al., Particle data group. Review of particle physics. Chin. Phys. C **40**(10), 421–428 (2016). https://doi.org/10.1088/1674-1137/40/10/100001
9. Y.-C. Wu, X.-Q. Hao, Q. Yue et al., Measurement of cosmic ray flux in the China JinPing underground laboratory. Chin. Phys. C **37**, 086001 (2013). https://doi.org/10.1088/1674-1137/37/8/086001
10. J. Su, Z. Zeng et al., Monte Carlo simulation of muon radiation environment in China Jinping Underground Laboratory. High Power Laser Part. Beams 24 **2012**(12), 3015–3018 (2012). https://doi.org/10.3788/HPLPB20122412.3015
11. V.A. Kudryavtsev, Muon simulation codes MUSIC and MUSUN for underground physics. Comput. Phys. Commun. **180**(3), 339–346 (2009). https://doi.org/10.1016/j.cpc.2008.10.013
12. T.K. Gaisser, R. Engel, E. Resconi, *Cosmic Rays and Particle Physics*, 2nd edn. (Cambridge University Press, Cambridge, 2016), pp. 1–29. https://doi.org/10.1017/CBO9781139192194
13. S. Agostinelli et al., Geant4-a simulation toolkit. Nucl. Instrum. Methods Phys. Res. Sect. A Accel. Spectrom. Detect. Assoc. Equip. **506**(3), 250–303 (2003). https://doi.org/10.1016/S0168-9002(03)01368-8

14. J.J. Back, Y.A. Ramachers, ACTIVIA: calculation of isotope production cross-sections and yields. Nucl. Instrum. Methods Phys. Res. Sect. A Accel. Spectrom. Detect. Assoc. Equip. **586**, 286–294 (2008). https://doi.org/10.1016/j.nima.2007.12.008
15. Q. Hu, H. Ma, Z. Zeng et al., Neutron background measurements at China Jinping underground laboratory with a Bonner multi-sphere spectrometer. Nucl. Instrum. Methodds A **859**, 37–40 (2017). https://doi.org/10.1016/j.nima.2017.03.048